Quantifying the economic value of space weather forecasting for power grids: an exploratory study

J. P. Eastwood,[1] M. A. Hapgood,[2] E. Biffis,[3] D. Benedetti,[3] M. M. Bisi,[2] L. Green,[4] R. D. Bentley,[4] and C. Burnett,[5]

[1.]The Blackett Laboratory, Imperial College London, London SW7 2AZ, UK

[2.] RAL Space, STFC Rutherford Appleton Laboratory, Harwell Campus, Didcot, Oxfordshire, OX11 0QX, UK

[3.] Department of Finance, Imperial College Business School, Imperial College London, London SW7 2AZ, UK

[4.] Mullard Space Science Laboratory, Holmbury St. Mary, Dorking, Surrey, RH5 6NT, UK

[5.] Space Weather Programme, Met Office, FitzRoy Road, Exeter EX1 3PB, UK

SHORT TITLE: ECONOMETRIC MODELING OF SW ECONOMIC IMPACT

Key points

- Physics-based frameworks are one way to assess the economic impact of space weather for policy and risk management
- A methodology based on substorms, and including forecast quality, is proposed to model geomagnetic storm impact.
- 1-in-10, -30, and -100 year scenarios are developed and example calculations of economic impact are presented.

Abstract

An accurate understanding of space weather socio-economic impact is fundamental to the development of appropriate operational services, forecasting capabilities, and mitigation strategies. One way to approach this problem is by developing physics-based models and frameworks that can lead to a bottom-up estimate of risk and likely impact. Here we describe the development of a new framework to assess the economic impact of space weather on power distribution networks and the supply of electricity. In particular, we focus on the phenomenon of the geomagnetic substorm, which is relatively localised in time and space, and occurs multiple times with varying severity during a geomagnetic storm. The framework uses the AE index to characterise substorm severity, and the impact of the substorm is modulated by the resilience of the power grid and the nature of available forecast. Possible scenarios for substorm sequences during a 1-in-10, a 1-in-30 and a 1-in-100 year geomagnetic storm event are generated based on the 2003, 1989, and 1859 geomagnetic storms. Economic impact, including international spill-over, can then be calculated using standard techniques, based on the duration and the geographical footprint of the power outage. Illustrative calculations are made for the European sector, for a variety of forecast and resilience scenarios. However, currently available data is highly regionally inhomogeneous, frustrating attempts to define an overall global economic impact at the present time.

Index Terms

4305 Space weather (2010, 2788, 7900)

4336 Economic impact of disasters

2790 Substorms

7954 Magnetic storms

7959 Models

1. Introduction

The need for a stable, reliable supply of electricity lies at the heart of modern society. The primary terrestrial risk attached to space weather is therefore its impact on conducting ground infrastructure, specifically power distribution networks [e.g., *Cannon et al.*, 2013; *Eastwood et al.*, 2017a; *Hapgood*, 2010; *Lloyd's*, 2013; *Oughton et al.*, 2017; *Schrijver et al.*, 2015]. The primacy of security of power supply is recognised, for example, by the fact that several major meetings have been organised on this subject in the past few years [e.g., *Showstack*, 2011]. Furthermore, space weather is now included in lists of events and phenomena that may have a worldwide economic impact as documented by the OECD and the World Economic Forum [*Howell*, 2013; *OECD*, 2011].

Although space weather generates a multitude of impacts and risk factors, geomagnetic activity is by far the most relevant for power distribution systems. The Earth's magnetic field forms the magnetosphere, whose dynamics are strongly driven by the solar wind [e.g., *Eastwood et al.*, 2017b]. This mainly depends on the strength and orientation of the interplanetary magnetic field and the solar wind speed. Magnetic reconnection allows energy and solar wind plasma to enter the magnetosphere on the dayside; energy is stored and explosively released on the nightside. The elemental response of the magnetosphere is the geomagnetic substorm, which occurs periodically in response to intervals of southward IMF in the solar wind and notably produces vivid auroral displays at high latitudes. Strong prolonged driving of the magnetosphere can lead to the development of a geomagnetic storm. Within geomagnetic storm intervals, power grids are affected by ground induced currents (GICs), driven by storm-generated geo-electric fields, which are induced by rapidly changing magnetic fields at and within the Earth's surface (dB/dt) [e.g., *Viljanen et al.*, 2006].

GICs may impact power grids in three ways [e.g., *Cannon et al.*, 2013 and references therein]: they may damage the physical infrastructure (specifically transformers, although this also depends on the transformer design), they may introduce voltage instability which could lead to a blackout without damaging the infrastructure, and they may interfere with the operation of protection systems and fault detection. The severity of a GIC impact is often measured or monitored according to the local rate of change of the horizontal geomagnetic field dB/dt, on time-scales of seconds to minutes [*Beamish et al.*, 2002]. In the UK, passing the threshold of 500 nT/min would constitute a GIC impact with possible adverse impact [*Cannon et al.*, 2013; *Erinmez et al.*, 2002]. A 1 in 100 year event may exhibit changing magnetic fields as large as 5000 nT/min [*NERC*, 2010; *Thomson et al.*, 2011].

There are many documented impacts of space weather on power grids. For example, in the UK two transformers were damaged during the 13 March 1989 storm [*Erinmez et al.*, 2002; *Smith*, 1990]. *Thomson et al.* [2005] examined the impact on the Scottish power grid of the 2003 storms and described how the models presented in the paper were being used to monitor, warn and analyse the properties of GICs. Distortion of the magnetising current causing harmonics which interfere and possibly trigger protective relays have been detected in the UK national grid on 14 July 1982, 13-14 March 1989, 19-20 October 1989 and 8 November 1991 [*Cannon et al.*, 2013].

The impact on continental Europe has been examined at regional level particularly focussing on high latitudes, for example Finland [*Juusola et al.*, 2015; *Pirjola et al.*, 2005]. The impact of the 2003 storms on the Swedish high voltage power transmission system are reported by *Pulkkinen et al.* [2005]. In this case, a 90 minute blackout left 50,000 customers without power in southern Sweden. This blackout arose because of protective relays being erroneously triggered [*Cannon et al.*, 2013]. GICs have also been reported at mid-latitudes,

96 e.g. in Spain and Europe more generally as part of the FP7 EURISGIC project [*Torta et al.*,
97 2012; *Viljanen*, 2011].

98 In North America, the impact of the 1989 geomagnetic storm on the Quebec power grid and
99 its failure is described in detail by *Bolduc* [2002]. This blackout arose also from the triggering
100 of protective relays [*Cannon et al.*, 2013]. A detailed technical assessment by Metatech Corp.
101 examining the wider impact of geomagnetic storms on the North American power grid
102 [*Kappenman*, 2010] includes a specific assessment of the 1989 event. In addition, an analysis
103 of power grid performance data by *Forbes and St Cyr* [2012] examined whether power
104 system reliability was challenged regionally in the United States during solar cycle 23 and
105 concludes that "geomagnetic activity can significantly increase the likelihood that the system
106 operator will dispatch generating units based on system stability considerations rather than
107 economic merit." Adverse impacts on the US power grid between 1992 and 2010 have also
108 been analysed by *Schrijver and Mitchell* [2013]. They conclude that 4% of the disturbances
109 reported to the US Department of Energy are attributable to strong geomagnetic activity. A
110 further study by *Schrijver et al.* [2014] suggests that space-weather-induced variations in the
111 quality of electric power lead to around 500 insurance claims per year in the US for
112 equipment malfunctions due to power supply problems.

113 Although the majority of the literature focuses on North America and Europe, other regions
114 have been investigated. The impact on South Africa has been studied by a number of authors
115 [e.g., *Lotz and Cilliers*, 2015 and references therein; *Matandirotya et al.*, 2015]. Of particular
116 importance here is the work by *Gaunt and Coetzee* [2007]. The impact of GICs in Japan has
117 been studied for example by *Watari* [2015]. Similarly, GIC impact in China has been
118 reported by *Wang et al.* [2015]. The impact of GICs on the Brazilian power system has been
119 reported by *Trivedi et al.* [2007], based on measurements since early 2004 (motivated in part
120 by the impact in South Africa of the 2003 geomagnetic storms).

121 The economic impact of any hazard is a function of the i) spatial and temporal extent of the
122 hazard, ii) the vulnerability of the technologies/infrastructures susceptible to failure, iii) the
123 degree of mitigation (backup generation), iv) and input production and consumption options
124 available to firms and consumers. It has been argued that a 1 in 100 year event (i.e.
125 Carrington class, such as the 1859 space weather event [*Stewart*, 1861]) could lead to
126 catastrophic impact, with damage to transformers taking a considerable length of time (years)
127 to recover from, and a consequent economic impact in the trillions of dollars range because of
128 the lack of power for a very prolonged period of time [*Kappenman*, 2010]. In such a scenario,
129 it has been calculated that the worldwide direct and indirect losses from a Quebec-like space
130 weather event whose outage is extended to one year would range 'from $2.4 trillion - $3.4
131 trillion over a year' [*Schulte in den Baeumen et al.*, 2014]. In contrast, the 2012 North
132 American Electric Reliability Corporation report [*NERC*, 2012] finds that the more likely
133 impact is system collapse due to voltage instability. In this case the outage would be
134 measured in hours to days, rather than months. This is mirrored in the opinion of the UK
135 impact report by *Cannon et al.* [2013] who conclude that the current worst case estimate for
136 the impact of a Carrington-class event on the UK power grid is for some local blackouts due
137 to voltage instability lasting a few hours, and damage to "super grid" transformers (an
138 approximate estimate of around 6 in England and Wales, 7 in Scotland). More recently,
139 *Gaunt* [2014] has shown that there are still considerable uncertainties in our understanding of
140 the potential of GIC to damage transformers. Thus we consider short-term blackouts as a
141 clear lower bound for the grid impacts that we consider here. Such blackouts lasting even a
142 few days can have a considerable economic impact. For example, the economic impact of the
143 14 August 2003 northeast blackout was estimated to be $4 - $10 billion [*US - Canada Power*
144 *System Outage Task Force*, 2006], with a more refined estimate using input-output modelling
145 of $6.53 billion [*Anderson et al.*, 2007]. Whilst this blackout was due to bad weather and a

failure to control vegetation near power lines, it provides a good way to cross-calibrate estimates of space weather economic impacts.

The Cambridge Centre for Risk Studies study of the economic impact of a severe space weather event focusses largely on the impact to the US power grid [*Oughton et al.*, 2016]; see also *Oughton et al.* [2017]. This model indicates a loss of US GDP between $135 - $610 billion over a 5-year period following the space weather event, with the worst affected states being Illinois and New York. It also indicates significant knock-on impacts to the global economy with China, Canada and Mexico being worst affected (as they are the US' largest trading partners), but also significant impacts on the UK, Japan and Germany.

Finally, a recent study[1] commissioned by the European Space Agency's Space Situational Awareness program performed by PricewaterhouseCoopers provides a cost-benefit analysis of the Space Weather (SWE) programme [*ESA*, 2016]. The 'best educated estimate' of the impact is a blackout affecting three cities for three days in the case of a G5-G5+ event. By modelling this impact on three 'average' European cities (i.e. geographically non-specific), and assuming the current space weather monitoring capability is available, the cost is found to be €5.771 billion. The impact of morbidity and power infrastructure damage is also accounted for.

As a matter of public policy, there is therefore considerable interest in understanding the economic risk of space weather, and therefore an econometric framework is required that is strongly grounded in the underlying physical phenomena. Furthermore, to be useful as a policy tool, it is also necessary to understand the feedback of investment to address the space weather risk. The purpose of this article is to report the development of a new econometric framework developed from the ground up. Two key aspects are as follows. The first is to use

[1] https://www.esa.int/About_Us/Business_with_ESA/GSEF/A_cost-benefit_analysis_of_the_SSA_programme

169 a substorm-based approach, rather than Dst or Kp. The second is to characterise the impact of
170 improved situational awareness, manifested as a reduction in the impact footprint. The
171 approach is designed to be modular and scalable, with flexibility built in at several levels,
172 allowing for a range of forecast outcomes based on adjusting model parameters.

173 The work is organised as follows. Our methodology, which is based on the construction of
174 substorm time series, is described in Section 2. The impact of a particular substorm on a
175 particular geographic region is a function of the substorm severity, the resilience of the
176 network (i.e. its ability to recover from an external disruptive event [*Henry and Emmanuel*
177 *Ramirez-Marquez*, 2012; *Pant et al.*, 2014]) and the quality of the forecast. This leads to a
178 projected outage impact. Evidently the precise decisions used here are, to some extent,
179 subjective, but we emphasise the importance of the framework in allowing different
180 parameters to be adjusted leading to a range of forecasted impacts, which furthermore can be
181 explored by re-categorising substorms, networks, and forecast quality. Section 3 then uses
182 historic data from the 1989, 2003 and 1859 storms to construct 1-in-10, 1-in-30 and 1-in-100
183 year scenarios. Section 4 examines how this data can be translated into a calculation of
184 economic impact, and focusses on the building block of the model, an individual substorm,
185 here modelled over Western Europe. Finally Section 5 provides a discussion of the current
186 obstacles to the full implementation of the framework model, and proposals for future work.

187 **2. Methodology**

188 One conclusion to be drawn from the documented impact of space weather is that this does
189 not simply depend on geophysical characteristics. It also depends on the properties of the
190 network (its resilience) and the quality of the available forecast. For example the National
191 Grid in the UK is particularly aware of the impact on large "super grid" transformers which
192 reduce the voltage from the transmission system to the local distribution networks [*Cannon et*

193 *al.*, 2013]. Consequently, models should account for both the physical driver and the system
194 response. In their study of economic impact, [*Oughton et al.*, 2016] defined an innovative
195 parameterisation of grid impacts that has allowed the authors to explore a range of
196 possibilities, reflecting different expert views on grid susceptibility. In particular, it included
197 lower and higher estimates of the level of disruption and damage to critical grid hardware
198 such as transformers, as well as a range of recovery times. It also resolves impacts to the level
199 of individual US states taking account of geomagnetic latitude, ground conductivity and the
200 number of transformers in each state.

201 In developing the present physics-based framework that treats substorms and GICs as the
202 primary risk to power grids, we propose that the impact depends on three key factors: (1) the
203 size of the physical driver; (2) the resilience of the grid; (3) the quality of the forecast. The
204 first two factors are self-evident, and are discussed in section 2.1 and 2.2 below. The final
205 factor is included to account for the reasonable assumption that the quality of the space
206 weather information available to a grid operator will make a material difference to their
207 operational response, and thus reduce the size of the impact. We consider three levels of
208 forecast quality: 'No Forecast', in which there is no L1 coronagraph or solar wind data;
209 'Current Forecast', in which there are the currently available assets and forecasts; and
210 'Improved Forecast', where an augmented space-based monitoring system with spacecraft at
211 the Sun-Earth L1 and L5 Lagrange points is available. This is discussed further in section 2.3,
212 and the mapping of the physical driver to its impact is discussed in section 2.4.

213 **2.1 Quantification of the physical driver**

214 Although the precise relationship between substorms and storms remains unclear and a topic
215 of active research, most operational space weather services focus on the incidence of storms,
216 and characterise their severity on an intensity scale from 1 (weakest) to 5 (strongest); this is

derived from the Kp index (Kp_{max} = 9) [*Bartels et al.*, 1939]. However, since Kp captures the severity of the global perturbation to the quiet magnetic field, it is not directly useful for understanding the most important societal impact – the production of GICs that may affect power grids. Consequently, a simple probabilistic statement that a G5 storm has a certain chance of causing a blackout does not necessarily contain the essential physics that controls the underlying behaviour. A more appropriate index is arguably the AE index, used to characterise the ground magnetic field perturbation caused by substorms through the currents generated by the aurora [*Davis and Sugiura*, 1966]. Substorm related fluctuations have been identified as the drivers of major impacts [*Fiori et al.*, 2014; *Villiers et al.*, 2017], not least the events of 1989 and 2003 described above, as well as earlier events in 1982 (UK/Sweden) and 1972 (US) [*Lanzerotti*, 1992]. Whilst this is not yet used in the operational domain, it is widely used scientifically, and data are easily available. It also has the advantage of being compatible with regional forecasting, which is a goal of agencies currently tasked with forecasting space weather.

Although GICs are mainly created at high latitudes by the electrical ionospheric currents caused by substorms and are regionally located on scales of 500-1000 km [*Ngwira et al.*, 2013; *Pulkkinen et al.*, 2015] they can be produced by other mechanisms. We note that: (a) the initial compression of the magnetosphere by interplanetary shocks can also drive GICs both in equatorial regions [*Carter et al.*, 2015], and at mid- and low latitudes [*Kappenman*, 2003; *Marshall et al.*, 2012]; (b) changes in the ring current can drive GICs in low latitude regions [*Gaunt and Coetzee*, 2007]. Consequently, by constructing a framework based on substorms, it will be possible, as our understanding progresses, to fit this into the wider understanding of geomagnetic storm activity in a robust and sensible way, alongside other storm effects. Here we describe the intensity of substorms qualitatively: Very intense (AE > 1900 nT); Intense (1500< AE <1900 nT); High (1200< AE <1500 nT); Moderate (500< AE

242 <1200 nT). Note that we do not consider events with AE < 500 nT. The motivation for using
243 these categories is discussed in Section 2.4 below.

244 ## 2.2 Grid resilience

245 The second dimension is the resilience of the network itself to space weather. In table 1 we
246 provide an initial assessment of a possible characterisation of grid resilience. This represents
247 the simplest possible characterisation at a very coarse level – is the grid resilience high or
248 low? This depends on: (a) the geographic location of the network; (b) the structure of the
249 network; (c) the typical stress on the network; (d) any use of transformers and other
250 equipment that is more space-weather resilient; (e) the perceived engagement from the
251 system operator.

252 ## 2.3 Forecast quality

253 The three forecast scenarios (no forecast/ current forecast/ improved forecast) are defined as
254 follows:

255 • No forecast available. This reflects a position where existing satellite observing
256 systems are not replaced prior to the end of their operational life expectancy or at the
257 end of the scientific mission for which they were originally intended.
258 • The current level of forecast. Currently forecasting relies on data from multiple
259 satellites including the Deep Space Climate Observatory (DSCOVR), the Solar and
260 Heliospheric Observatory (SOHO), and the Advanced Composition Explorer (ACE)
261 all located in the vicinity of the first Sun-Earth Lagrange point (L1), and
262 Geostationary Operational Environmental Satellite (GOES) and Solar Dynamic
263 Observatory (SDO) in Earth orbit.
264 • Improved level of forecasting. Reflecting the standard that could be achieved if the
265 current observation satellites were supplemented by satellites off the Sun-Earth line,

as demonstrated by the STEREO mission e.g. at the fourth and fifth Sun-Earth Lagrange points (L4 and/or L5) [e.g., *ESA*, 2016]. Although there have been projects to address in situ measurements of the solar wind from sub-L1 [*Eastwood et al.*, 2015], any realistic, near-term, improved, operational system will rely on measurements from L1 and L5. Even though this improved system would not offer a specific improvement in the knowledge of the magnetic field orientation upstream of the Earth, the value of imaging the Sun away from the Sun-Earth line, and the knowledge of the solar wind conditions provides actionable information which end users will use to maximise preparedness.

2.4 Mapping the physical driver to the impact

The impact severity depends on substorm strength, power grid resilience and forecast quality. The severity and the resilience combine to set the level of the overall impact. The level of the available forecast may change both the level of the impact and its duration. Table 2 summarises the estimated impact severity based on these three factors. Here the impact table is informed by the analysis in the Royal Academy of Engineering report [*Cannon et al.*, 2013].

The calibration of qualitative substorm intensity and impact is defined by reports of major GIC impacts. Very intense substorms caused the impacts experienced in the UK and Quebec during the March 1989 storm (see Figure 1a). Another very intense substorm early on 14 July 1982 (not shown) caused loss of power in parts of Scotland [*Beamish et al.*, 2002] and rail signal disruption (green lights turned red) in Sweden [*Wik et al.*, 2009]. An intense substorm just after 21:00UT on 13 March 1989 (Figure 1a) also caused an alarm on a UK transformer, whilst an intense substorm around 20:00UT on 30 October 2003 (Figure 1c) caused a loss of power in Malmö in Sweden [*Wik et al.*, 2009]. These events give confidence that the

290 substorm classes of intense and very intense indicate a potential for disruptive levels of GIC
291 in power grids and rail systems, especially at upper middle latitudes (45° - 60°). This
292 approach is also consistent with the analysis in the Royal Academy of Engineering report of
293 space weather impacts on engineered systems [*Cannon et al.*, 2013]. The lower end of our
294 scale of substorm classes and their impacts is then set by scaling down the impacts from the
295 higher end of the scale. For high resilience power grids this scaling down is simply that we
296 expect zero impact from the lower substorm classes. For less resilient grids, our scaling down
297 allows for minor impacts from events in our third substorm class (high). Here resilience
298 arises from several factors including (a) the hardening of grid assets, such as transformers, to
299 withstand substantial GICs; and (b) good awareness of the risk, so that the grid operator is
300 ready to ensure grid stability (e.g. through provision of additional reactive power) during a
301 severe space weather event.

302 The impact severity has been scaled so that this declines with increasing forecast capability.
303 A key assumption we make is that better forecasts improve the speed of recovery, since the
304 recovery management process can be better prepared for [*Cabinet Office*, 2015]. Much of the
305 economic impact arises from the disruption of productive activities over the recovery period,
306 rather than from the immediate impact of the space weather event (a substorm in our
307 framework). Thus our framework provides a scaling of recovery times that allows us to
308 compare different forecast schemes. For the present study we have assigned what we consider
309 to be realistic recovery times, based for example on recovery times for other grid impacts and
310 other studies [*Cannon et al.*, 2013]. This scaling is easily adjustable and could be refined if
311 future work were to indicate that these recovery times were not optimal for the analysis.

312 **3. Construction of power grid impact scenarios**

To quantify the global impact of a major space weather event, it is useful to consider the likely sequence of events that may occur during a 1-in-10, 1-in-30 and 1-in-100 year event. Candidate scenarios can be based around the March 1989 (1-in-30), Carrington (1-in-100) and October 2003 (1-in-10) events, as we now describe. This order reflects the logical process through which we developed and normalised the scenarios, with the 1-in-100 year scenario building on the 1-in-30 year scenario, whilst the 1-in-10 year scenario is independent of the other two. In particular, we begin with the 1989 event as this is, to date, the one which had the largest documented impact in the modern era.

3.1 1-in-30 year event

This scenario is derived from the observations of the great geomagnetic storm of 13-14 March 1989, shown in Figure 1a. Substorms were identified by taking the 31-minute running median of 1-min resolution AE index data, and then picking relevant maximum and minima by automated analysis. The AE index is shown in Figure 1. The initial impact longitude is assumed to be at 2.5 hours local time, reflecting experience from the 1989 storm where major grid impacts in Canada and the UK occurred during this event (but on different days). This initial impact longitude is used in all three scenarios. The qualitative intensity of each substorm is defined as moderate, high, intense and very intense according to the definitions given in Table 1. Over a two-week period of intense space weather centred on this storm, 85 substorms were calculated to have occurred. Supporting Information Table 1 shows a subset of these substorms: those occurring during periods when geomagnetic activity reached or exceeded G1 intensity. Note that here we also identify secondary impact areas for the intense and very intense events, allowing for the possibility of a spread in impact longitude (and perhaps also a spread to lower latitudes).

3.2 1-in-100 year event

337 This scenario builds a simulated substorm sequence for a Carrington-class event. It is derived
338 from the observations of the great geomagnetic storm of March 1989; it takes the substorm
339 sequence from that event and replicates it twice so that we have two sets of substorms
340 matching the two geomagnetic storm periods noted in Balfour Stewart's 1861 paper on the
341 Carrington event [*Stewart*, 1861]. Thus where a substorm was observed in 1989 at time Δt
342 relative to the sudden storm commencement (SSC) that started the 1989 event, we replicate it
343 twice in the 1-in-100 year scenario: (a) first at time Δt relative to the first SSC reported by
344 Balfour Stewart and (b) second at time Δt relative to the second SSC reported by Balfour
345 Stewart. In addition to this mapping in time, the intensity of all substorms in dataset (b) is
346 increased by a factor of 1.44 to reflect the higher intensity of the Carrington storm; this factor
347 of increase represents the relative storm intensities as estimated from the Dst index: -589
348 measured in 1989 and -850 estimated for the second storm in 1859 [*Siscoe et al.*, 2006].Thus
349 the scenario identifies a long sequence of bursts of activity (substorms) that may be taken as
350 indicative of a Carrington-class event and includes estimates of where on Earth these would
351 have had their prime impact. The simulated sequence consists of 127 substorms and is shown
352 in Figure 1b. Supporting Information Table 2 shows the results of this analysis for the high,
353 intense and very intense strength substorms.

354 **3.3 1-in-10 year event**

355 The 1-in-10 year event scenario builds on the substorm sequence derived from observations
356 of the Halloween geomagnetic storm of October 2003. But to ensure consistent scaling with
357 the two scenarios above, we adjusted the 2003 AE data downward by a factor of 0.62. This
358 factor reflects the lower intensity of the 2003 storm as estimated from the Dst index: -589
359 measured at 14/Mar/1989 01:00UT and -383 measured at 30/Oct/2003 22:00UT. It is applied
360 so that the peaks of smoothed AE adjacent to the times of minimum Dst (2011 at
361 14/Mar/1989 02:05UT and 2113 at 30/Oct/2003 19:59UT) are proportionally scaled. Having

made this adjustment, the methodology is the same as for the previous scenario and the substorm time series is shown in Figure 1c. Supporting Information Table 3 summarises the resulting set of substorm occurrence, duration, severity, impact longitude and primary target region. Note that only high, intense and very intense substorms are listed.

4. Economic analysis: proposed methodology and illustrative examples

4.1 Methodology

The next step in the analysis is to develop a model of the economic impact. Granularly capturing the various dimensions of economic impact is challenging, but we attempt it by using a combination of reduced form information on grid resilience for points ii) and iii) listed in the introduction and detailed spatio-temporal information on blackouts and Value-of-Lost-Load estimates at location for points i) and iv). Initially, this requires an approach to determine the economic impact of a single substorm of given duration and intensity, at a particular location on the globe. In addition to the different impact scenarios, we have also considered three different recovery periods, described as: i) immediate recovery, defined as recovery immediately after the duration of occurrence of each substorm; ii) no recovery, defined as zero recovery before the end of the specific disruption period indicated in the impact tables shown in Table 3; iii) linear recovery, defined as uniform recovery from the end of each substorm occurrence to the end of the recovery period indicated in the impact tables shown in Table 2. Although other non-linear recovery rules could have been used to characterize the power system behaviour between the immediate and no recovery case, a simple linear recovery rule provides a reasonable benchmark for intermediate forms of system resilience. Resilience can be inherent (e.g., good system design including the design of physical infrastructure, as well as capabilities to reallocate resources and adjust to the conditions) or adaptive (e.g., extra ingenuity/effort exerted in crisis situations – in which case

386 nowcasting can play a key role), and in the context of electricity disruptions resilience can
387 take the form of lower energy utilization per unit of output, fuel substitution, use of
388 alternative generation sources, production rescheduling, etc. [see *Rose et al.*, 2007]. Some
389 studies show that direct business resilience is quite high and can result in damage estimates
390 considerably lower than when resilience is ignored [e.g., *Rose and Liao*, 2005]. The
391 immediate recovery assumption can be thought as a proxy for a situation where both adaptive
392 and inherent resilience are fully at play.

393 To quantify the economic impact itself, we focus on Value of Lost Load (VoLL) as a loss
394 metric, quantifying both direct economic losses, such as production losses in different
395 industries, and indirect costs resulting from business interruption and opportunity costs from
396 power outage [*Coll-Mayor et al.*, 2012; *de Nooij et al.*, 2007; *Leahy and Tol*, 2011; *Tol*,
397 2007]. The empirical literature shows considerable variations in VoLL estimates, due to the
398 highly skewed distribution of values from households to different industry sectors and the
399 different estimation methodologies that can be used. As VoLL is not traded, it must be
400 estimated either with a structural model (production-function approach) or by eliciting market
401 participants' preferences via empirical evidence on consumer choices during power outages
402 (revealed preference model) or questionnaires and contingent valuation surveys (stated
403 preference models). Given our interest in forecasting, we find the last-mentioned approach
404 suitable for our analysis. Willingness-to-pay (WTP) to avoid an outage and Willingness-to-
405 accept (WTA) payment for an outage [*Lehtonen and Lemstrom*, 1995] are usually used to
406 estimate consumers' VoLL. We acknowledge the disparity of results on WTP/WTA available
407 in the literature, and therefore our analysis is based on a range of possible VoLL estimates,
408 but is ultimately calibrated to produce median estimates consistent with the European
409 Blackout simulator for UK and continental European exposures. The simulator is presented in
410 *Schmidthaler and Reichl* [2016]; see also discussions in the Royal Academy of Engineering

411 study on electricity shortfalls [*Royal Academy of Engineering*, 2014] and *Schmidthaler et al.*
412 [2015]. The blackout simulator is used to quantify each substorm's direct economic cost at
413 location. Residual, longer term power outage or reduced system capacity are not considered
414 in the estimates. As such, the latter can be interpreted as a lower bound for the economic
415 losses associated with the impact table (Table 2). In this paper, the occurrence of direct power
416 outage not recovered within 48 hours is restricted to the case of low-resilience locations
417 affected by the very intense substorm #41 (see Table 2). In those instances, we extrapolate
418 linearly the direct economic costs pertaining to the relevant areas.

419 To provide an assessment of international spillover we use Input-Output (IO) methodology
420 [e.g., *Haimes et al.*, 2005; *Miller and Blair*, 2009], aggregating the cross-sectoral
421 international impact of European power outages originating during the different substorms
422 illustrated above (see Supporting Information for further details with reference to *Haimes*
423 *Yacov and Jiang* [2001]; *Leontief* [1951]; *Santos and Haimes* [2004]). In line with the
424 existing literature, we rely on the 2011 Multi-Regional Input-Output table sourced from the
425 World Input-Output Database (WIOD). The IO methodology is well known to exaggerate
426 indirect losses as it allows for unidirectional impacts, while the combination of partial and
427 general equilibrium effects is more complex, in particular due to the resilience of a system. In
428 line with our above discussion on the concept of resilience, the existing literature suggests
429 that damage reduction can be considerable [e.g., *Rose and Liao*, 2005], but on the other hand
430 indirect (general equilibrium) costs can raise costs significantly [e.g., *Rose and Liao*, 2005].
431 Our application of IO analysis tries to capture some of these effects in reduced form and
432 conservatively, providing indirect costs that are on average 30% lower than application of the
433 standard model.

434 **4.2 An individual substorm**

435 To illustrate the proposed approach, here we consider the impact of a single "high intensity"
436 substorm affecting Western Europe (excluding Ireland and UK) and Scandinavia for 1 hours
437 and 9 minutes (substorm #21 in the 1-in-10 year scenario presented in Section 4.3 and
438 Supporting Information Table 3; the geographic footprint in continental Europe is shown in
439 Figure 2a). We estimate the economic costs by allowing for the low and high resilience of the
440 two geographic areas. Specifically, in this model Scandinavia experiences no impact
441 irrespective of forecast. Western Europe experiences either no impact (improved forecast) or
442 a limited power outage (2%) recovered in 48 hours (no forecast) or 24 hours (current
443 forecast). This leads to the results reported in Table 3 for different recovery and forecast
444 assumptions summarised in Table 2, modulated by the recovery profile. Under current
445 forecast conditions and linear recovery, an estimated economic impact of €170 million is
446 found.

447 It is instructive to break down these losses into different sectors. This is shown in Table 4.
448 Note that we aggregate sectors in line with the classification used in the European blackout
449 simulator [*Schmidthaler and Reichl*, 2016]. With Western Europe and Scandinavia being the
450 focus of the event, it is manufacturing that experiences the most significant losses.

451 Turning to international spill-over costs, these are reported in Table 5, again for different
452 recovery and forecast assumptions. For current forecast conditions and linear recovery, this is
453 calculated to be €22 – €32 billion. Table 5 demonstrates the sensitivity of this calculation to
454 the initial cost calculation in Table 3. In the case of no forecast and no recovery until the end
455 of the specified period after the substorm, the international spill-over estimate is €359 – 506
456 billion. On the other hand, if the forecast quality is sufficient to ensure no direct impact, then
457 evidently there would be no indirect impact either.

458 **4.3 Towards a comprehensive cost model**

459 The next level of complexity is to consider multiple substorms. To illustrate this, we examine
460 the 1-in-30 year scenario and consider substorms #28 and #41 (see Supporting Information
461 Table 1). Substorm #28 was a high intensity event, with a geographic footprint shown in
462 Figure 2b, which started at 00:35 on day 1 and had a duration of 2 hours 10 minutes. It was
463 followed by event #41, a very intense substorm which started at 01:05 on day 2 and had a
464 duration of 2 hours 35 minutes. This substorm is modelled to have a very large geographic
465 footprint as shown in Figure 2c. Here we will simply treat the substorms independently: no
466 overlapping is assumed for the recovery periods pertaining to the two different substorms.
467 Also, no recovery feedback effects from previous substorm are assumed in our analysis.

468 The aggregate costs of the two substorms on Europe alone are reported in Table 6. The
469 numbers are considerably larger than in the previous scenario: for the current forecast/linear
470 recovery case, the direct cost is estimated to be € 9,340 million. This is driven by the impact
471 of the very intense substorm on a low resilience grid, where for the current forecast, we
472 model the impact as being of much longer duration. For example, the system capacity is
473 reduced by 4% and recovered in 5 months.

474 Table 7 reports the results broken down by sector. As before, manufacturing accounts for the
475 most significant losses, but for this severity of event households now experience the second
476 highest losses. Using Input-Output analysis, we quantify the indirect economic costs of the
477 two substorms by looking at cross-country and cross-sectoral spillovers. The economic costs
478 of the two substorms are reported in Table 8 and illustrate a significant difference between
479 the different types of forecast. For the current forecast/linear recovery case, the estimated
480 indirect cost impact is €787 – 1,108 billion. This represents global losses. The complete loss
481 of forecast capability results in a tenfold increase in costs across all sectors.

482 **5. Discussion and conclusions**

Although the proposed approach necessarily leads to very detailed scenarios, particularly in the most severe and long-lived events, we argue that such an approach is necessary to fully understand the complex impacts of space weather. The approach is deliberately conservative, in the sense that it is based around elemental events that are limited in spatial footprint and duration, but nevertheless this provides a way to comprehensively estimate and understand the impact of a complex space weather event. It also provides a pathway to examine the full range of space weather economic impacts, particularly from smaller events that may occur more frequently. This is related to a growing realisation that vulnerability may arise not simply due to rare but severe events, but also due to continuing degradation as a consequence of many smaller impacts [*Schrijver et al.*, 2015]. The analysis of section 4.2 shows that even isolated substorms causing a limited outage can have a significant economic impact. In the case of two substorms over western Europe, and for current forecast/linear recovery conditions, the direct cost is estimated to be € 9,340 million, with an estimated international spill-over costs in the range of €787 – 1,108 billion. We have also attempted to quantify the impact of improved forecasting, and adjustments to the impact recovery footprint or timescale can have a significant impact. For example, in the two substorm case with linear recovery, moving from the current to the improved forecasting scenario (approximately halving the physical impact footprint) reduces the economic impact by a factor of ~3 to €3.7 billion. It also reduces the spill-over cost by a factor of 4. The development of improved situational knowledge is therefore likely to have a very significant cost/benefit ratio.

In making policy decisions, these benefits are tensioned against the cost of developing and operating an improved forecast system. Such an analysis is beyond the scope of the present work as it depends on the unique circumstances of each entity tasked with mitigating space weather risk. However, we offer the following observations. The decision to pursue such a mission would depend not only on power grid impact, but also on all other sectors that are

affected by space weather. Furthermore, each sector has its own requirements for the timescale on which resilience is formally justified (in several cases this may be at the 1-in-100 or 1-in-200 year level). A recent ESA study provides an estimated cost of €502 m over 2016-2032 to enable an 'improved forecast' system [*ESA*, 2016].

It is evident that the multiplicative effects of many such events during a prolonged Carrington-type event have the potential to be extremely severe. However, the calculation of economic impact for the whole scenario cannot yet be performed with confidence for several reasons, and this indicates areas that require immediate further investigation.

- The analysis can only be performed with confidence if reliable data on power grid infrastructure and hence direct economic losses of sufficient quality and fidelity is available. Whilst the data for western Europe is relatively mature, we were unable to acquire the necessary data from other regions of the world to attempt a more comprehensive analysis.
- The recovery scenarios used here are relatively simple, but also can be adjusted or made more complex in response to improved knowledge about likely impact. In particular, the presence of other on-going space weather effects could impact the recovery and/or the operation of power networks. For example, it has recently been recognised by the UK government that space weather can also impact the power grid via GNSS [*London Economics*, 2017, page 51].
- Although the scenarios are derived from real observations, they are only representative. For example, shifting the onset time of each event by 6 hours would change the calculation significantly, since events that might happen in the United States would instead have their footprint over the Pacific Ocean. In the case of the 1-in-100 year scenario, the construction of the scenario is such that many of the most severe impacts occur over North America. This arises because we have used timings

from the 1859 Carrington event and is consistent with historical records from 1859 that report strong effects over the continental US such as disruption of telegraph systems and spectacular auroral displays, [e.g. see the collection of papers edited by *Clauer and Siscoe*, 2006]. For the 1-in-10 and 1-in-30 year scenarios, the effects are even more regionally located, and so it should be understood that a full analysis requires a Monte-Carlo type analysis where the timing, ordering, and intensity of the substorms are changed both systematically and randomly.

- Finally, the total cost of all these events is unlikely to combine linearly, and indeed it is not yet known how the knock-on effects should be treated. For example, a power outage is likely to cause knock-on effects in adjacent regions not captured here; it is not yet clear how this should modify the impact calculation. This becomes increasingly important as the complexity and duration of the scenario increases, evidently most so in the 1-in-100 year scenario.

Although construction of the total economic cost of a particular scenario should therefore be approached extremely carefully (and we do not attempt such a calculation here), investigation of these aspects building on the framework approach presented here will enable a more robust assessment of space weather economic impact and facilitate evidence-based policy decisions. Furthermore, we anticipate that this framework approach can also be applied to other space weather impacts in the future (e.g. aviation and GNSS).

Acknowledgements

Data is publicly available from the World Data Center for Geomagnetism, Kyoto (http://wdc.kugi.kyoto-u.ac.jp/aedir/), the International Service on Rapid Magnetic Variations (http://www.obsebre.es/en/rapid), the Blackout Simulator (http://www.blackout-

simulator.com) and the World Input Output Database (http://www.wiod.org/home). This work was funded by the U.K. Space Agency International Partnership Space Programme (collaboration agreement L2796). EB acknowledges useful discussions with Richard Green, and Malcolm Kemp/Nematrian.

561 **References**

562 Anderson, C. W., J. R. Santos, and Y. Y. Haimes (2007), A Risk-based Input–Output
563 Methodology for Measuring the Effects of the August 2003 Northeast Blackout, *Economic*
564 *Systems Research*, *19*(2), 183-204, doi:10.1080/09535310701330233.

565 Bartels, J., N. H. Heck, and H. F. Johnston (1939), The three-hour-range index measuring
566 geomagnetic activity, *J.Geophys.Res.*, *44*, 411-454.

567 Beamish, D., T. D. G. Clark, E. Clarke, and A. W. P. Thomson (2002), Geomagnetically
568 induced currents in the UK: geomagnetic variations and surface electric fields, *J. Atmos. Sol.-*
569 *Terr. Phys.*, *64*(16), 1779-1792, doi:https://doi.org/10.1016/S1364-6826(02)00127-X.

570 Bolduc, L. (2002), GIC observations and studies in the Hydro-Quebec power system,
571 *J.Atmos.Sol.Terr.Phys.*, *64*, 1793-1802.

572 Cabinet Office (2015), Space Weather Preparedness Strategy*Rep. BIS/15/457* UK
573 Government, Department for Business Innovation and Skills London.

574 Cannon, P., et al. (2013), Extreme space weather: impacts on engineered systems and
575 infrastructure*Rep. ISBN 1-903496-95-0*, Royal Academy of Engineering, London.

576 Carter, B. A., E. Yizengaw, R. Pradipta, A. J. Halford, R. Norman, and K. Zhang (2015),
577 Interplanetary shocks and the resulting geomagnetically induced currents at the equator,
578 *Geophysical Research Letters*, *42*(16), 6554-6559, doi:10.1002/2015gl065060.

579 Clauer, R. C., and G. Siscoe (2006), The great historical geomagnetic storm of 1859: A
580 modern look, *Advances in Space Research*, *38*(2), 117-118,
581 doi:https://doi.org/10.1016/j.asr.2006.09.001.

582 Coll-Mayor, D., J. Pardo, and M. Perez-Donsion (2012), Methodology based on the value
583 of lost load for evaluating economical losses due to disturbances in the power quality, *Energy*
584 *Policy*, *50*, 407-418, doi:https://doi.org/10.1016/j.enpol.2012.07.036.

585 Davis, T. N., and M. Sugiura (1966), Auroral electrojet activity index AE and its universal
586 time variations, *Journal of Geophysical Research*, *71*(3), 785-801,
587 doi:doi:10.1029/JZ071i003p00785.

588 de Nooij, M., C. Koopmans, and C. Bijvoet (2007), The value of supply security: The
589 costs of power interruptions: Economic input for damage reduction and investment in
590 networks, *Energy Economics*, *29*(2), 277-295,
591 doi:https://doi.org/10.1016/j.eneco.2006.05.022.

592 Eastwood, J. P., E. Biffis, M. A. Hapgood, L. Green, M. M. Bisi, R. D. Bentley, R. Wicks,
593 L. A. McKinnell, M. Gibbs, and C. Burnett (2017a), The Economic Impact of Space
594 Weather: Where Do We Stand?, *Risk Analysis*, *37*(2), 206-218, doi:10.1111/risa.12765.

595 Eastwood, J. P., D. O. Kataria, C. R. McInnes, N. C. Barnes, and P. Mulligan (2015),
596 Sunjammer, *Weather*, *70*(1), 27-30, doi:10.1002/wea.2438.

Eastwood, J. P., R. Nakamura, L. Turc, L. Mejnertsen, and M. Hesse (2017b), The Scientific Foundations of Forecasting Magnetospheric Space Weather, *Space Science Reviews*, *212*(3), 1221-1252, doi:10.1007/s11214-017-0399-8.

Erinmez, I. A., J. G. Kappenman, and W. A. Radasky (2002), Management of the geomagnetically induced current risks on the national grid company's electric power transmission system, *J. Atmos. Sol.-Terr. Phys.*, *64*(5-6), 743-756, doi:10.1016/s1364-6826(02)00036-6.

ESA (2016), SWE Cost Benefit Analysis*Rep.*, Paris.

Fiori, R. A. D., D. H. Boteler, and D. M. Gillies (2014), Assessment of GIC risk due to geomagnetic sudden commencements and identification of the current systems responsible, *Space Weather*, *12*(1), 76-91, doi:doi:10.1002/2013SW000967.

Forbes, K. F., and O. C. St Cyr (2012), Did geomagnetic activity challenge electric power reliability during solar cycle 23? Evidence from the PJM regional transmission organization in North America, *Space Weather-the International Journal of Research and Applications*, *10*, doi:10.1029/2011sw000752.

Gaunt, C. T. (2014), Reducing uncertainty – responses for electricity utilities to severe solar storms, *J. Space Weather Space Clim.*, *4*, A01.

Gaunt, C. T., and G. Coetzee (2007), *Transformer failures in regions incorrectly considered to have low GIC-risk*, 807-812 pp., doi:10.1109/pct.2007.4538419.

Haimes Yacov, Y., and P. Jiang (2001), Leontief-Based Model of Risk in Complex Interconnected Infrastructures, *Journal of Infrastructure Systems*, *7*(1), 1-12, doi:10.1061/(ASCE)1076-0342(2001)7:1(1).

Haimes, Y. Y., B. M. Horowitz, J. H. Lambert, J. R. Santos, C. Lian, and K. G. Crowther (2005), Inoperability Input-Output Model for Interdependent Infrastructure Sectors. I: Theory and Methodology, *Journal of Infrastructure Systems*, *11*(2), 67-79, doi:doi:10.1061/(ASCE)1076-0342(2005)11:2(67).

Hapgood, M. (2010), Space weather: its impact on Earth and implications for business*Rep.*, Lloyd's, London.

Henry, D., and J. Emmanuel Ramirez-Marquez (2012), Generic metrics and quantitative approaches for system resilience as a function of time, *Reliability Engineering & System Safety*, *99*, 114-122, doi:https://doi.org/10.1016/j.ress.2011.09.002.

Howell, L. (2013), Global Risks 2013 Eighth Edition, edited by W. E. Forum, World Economic Forum, Switzerland.

Juusola, L., A. Viljanen, M. van de Kamp, E. I. Tanskanen, H. Vanhamaki, N. Partamies, and K. Kauristie (2015), High-latitude ionospheric equivalent currents during strong space storms: Regional perspective, *Space Weather-the International Journal of Research and Applications*, *13*(1), 49-60, doi:10.1002/2014sw001139.

Kappenman, J. (2003), Storm sudden commencement events and the associated geomagnetically induced current risks to ground-based systems at low-latitude and

midlatitude locations, *Space Weather-the International Journal of Research and Applications*, *1*(3).

Kappenman, J. (2010), Geomagnetic storms and their impact on the US power grid*Rep.*, Metatech Corp.

Lanzerotti, L. J. (1992), Comment on "Great magnetic storms" by Tsurutani et al, *Geophysical Research Letters*, *19*(19), 1991-1992, doi:10.1029/92GL02238.

Leahy, E., and R. S. J. Tol (2011), An estimate of the value of lost load for Ireland, *Energy Policy*, *39*(3), 1514-1520, doi:https://doi.org/10.1016/j.enpol.2010.12.025.

Lehtonen, M., and B. Lemstrom (1995), Comparison of the methods for assessing the customers' outage costs, paper presented at Energy Management and Power Delivery, 1995. Proceedings of EMPD '95., 1995 International Conference on, 21-23 Nov 1995.

Leontief, W. W. (1951), Input-Output Economics, *Scientific American*, *185*(4), 15-21.

Lloyd's (2013), Solar Storm Risk to the North American Electric Grid*Rep.*, Lloyd's.

London Economics (2017), The economic impact on the UK of a disruption to GNSS*Rep.*, London Economics, London.

Lotz, S. I., and P. J. Cilliers (2015), A solar wind-based model of geomagnetic field fluctuations at a mid-latitude station, *Advances in Space Research*, *55*(1), 220-230, doi:10.1016/j.asr.2014.09.014.

Marshall, R. A., M. Dalzell, C. L. Waters, P. Goldthorpe, and E. A. Smith (2012), Geomagnetically induced currents in the New Zealand power network, *Space Weather*, *10*(8), doi:doi:10.1029/2012SW000806.

Matandirotya, E., P. J. Cilliers, and R. R. Van Zyl (2015), Modeling geomagnetically induced currents in the South African power transmission network using the finite element method, *Space Weather-the International Journal of Research and Applications*, *13*(3), 185-195, doi:10.1002/2014sw001135.

Miller, R. E., and P. D. Blair (2009), *Input-output analysis: foundations and extensions*, Cambridge University Press.

NERC (2010), High-impact, low frequency event risk to the north american power system*Rep.*, North America Electric Reliability Cooperation.

NERC (2012), Effects of geomagnetic disturbances on the bulk power system*Rep.*, North America Electric Reliability Corporation.

Ngwira, C. M., A. Pulkkinen, M. Leila Mays, M. M. Kuznetsova, A. B. Galvin, K. Simunac, D. N. Baker, X. Li, Y. Zheng, and A. Glocer (2013), Simulation of the 23 July 2012 extreme space weather event: What if this extremely rare CME was Earth directed?, *Space Weather*, *11*(12), 671-679, doi:10.1002/2013SW000990.

OECD (2011), Future Global Shocks. Improving Risk Governance*Rep.*, OECD.

672 Oughton, E. J., J. Copic, A. Skelton, V. Kesaite, J. Z. Yeo, S. J. Ruffle, M. Tuveson, A. W.
673 Coburn, and D. Ralph (2016), Helios Solar Storm Scenario*Rep.*, Centre for Risk Studies,
674 University of Cambridge Cambridge.

675 Oughton, E. J., A. Skelton, R. B. Horne, A. W. P. Thomson, and C. T. Gaunt (2017),
676 Quantifying the daily economic impact of extreme space weather due to failure in electricity
677 transmission infrastructure, *Space Weather*, *15*(1), 65-83, doi:10.1002/2016SW001491.

678 Pant, R., K. Barker, J. E. Ramirez-Marquez, and C. M. Rocco (2014), Stochastic measures
679 of resilience and their application to container terminals, *Computers & Industrial*
680 *Engineering*, *70*, 183-194, doi:https://doi.org/10.1016/j.cie.2014.01.017.

681 Pirjola, R., K. Kauristie, H. Lappalainen, A. Viljanen, and A. Pulkkinen (2005), Space
682 weather risk, *Space Weather-the International Journal of Research and Applications*, *3*(2),
683 doi:10.1029/2004sw000112.

684 Pulkkinen, A., E. Bernabeu, J. Eichner, A. Viljanen, and C. Ngwira (2015), Regional-scale
685 high-latitude extreme geoelectric fields pertaining to geomagnetically induced currents, *Earth*
686 *Planets and Space*, *67*, 1-8, doi:10.1186/s40623-015-0255-6.

687 Pulkkinen, A., S. Lindahl, A. Viljanen, and R. Pirjola (2005), Geomagnetic storm of 29-31
688 October 2003: Geomagnetically induced currents and their relation to problems in the
689 Swedish high-voltage power transmission system, *Space Weather*, *3*, S08C03-
690 doi:10.1029/2004SW000123.

691 Rose, A., and S.-Y. Liao (2005), Modeling Regional Economic Resilience to Disasters: A
692 Computable General Equilibrium Analysis of Water Service Disruptions*, *Journal of*
693 *Regional Science*, *45*(1), 75-112, doi:doi:10.1111/j.0022-4146.2005.00365.x.

694 Rose, A., G. Oladosu, and S.-Y. Liao (2007), Business Interruption Impacts of a Terrorist
695 Attack on the Electric Power System of Los Angeles: Customer Resilience to a Total
696 Blackout, *Risk Analysis*, *27*(3), 513-531, doi:doi:10.1111/j.1539-6924.2007.00912.x.

697 Royal Academy of Engineering (2014), *Counting the cost: The economic and social costs*
698 *of electricity shortfalls in the UK*, Royal Academy of Engineering, London.

699 Santos, J. R., and Y. Y. Haimes (2004), Modeling the Demand Reduction Input-Output (I-
700 O) Inoperability Due to Terrorism of Interconnected Infrastructures*, *Risk Analysis*, *24*(6),
701 1437-1451, doi:doi:10.1111/j.0272-4332.2004.00540.x.

702 Schmidthaler, M., J. Cohen, J. Reichl, and S. Schmidinger (2015), The effects of network
703 regulation on electricity supply security: a European analysis, *Journal of Regulatory*
704 *Economics*, *48*(3), 285-316, doi:10.1007/s11149-015-9277-z.

705 Schmidthaler, M., and J. Reichl (2016), Assessing the socio-economic effects of power
706 outages ad hoc, *Computer Science - Research and Development*, *31*(3), 157-161,
707 doi:10.1007/s00450-014-0281-9.

708 Schrijver, C. J., R. Dobbins, W. Murtagh, and S. M. Petrinec (2014), Assessing the impact
709 of space weather on the electric power grid based on insurance claims for industrial electrical
710 equipment, *Space Weather-the International Journal of Research and Applications*, *12*(7),
711 487-498, doi:10.1002/2014sw001066.

712 Schrijver, C. J., et al. (2015), Understanding space weather to shield society: A global road
713 map for 2015-2025 commissioned by COSPAR and ILWS, *Advances in Space Research*,
714 *55*(12), 2745-2807, doi:10.1016/j.asr.2015.03.023.

715 Schrijver, C. J., and S. D. Mitchell (2013), Disturbances in the US electric grid associated
716 with geomagnetic activity, *Journal of Space Weather and Space Climate*, *3*,
717 doi:10.1051/swsc/2013041.

718 Schulte in den Baeumen, H., D. Moran, M. Lenzen, I. Cairns, and A. Steenge (2014), How
719 severe space weather can disrupt global supply chains, *Natural Hazards and Earth System*
720 *Sciences*, *14*(10), 2749-2759, doi:10.5194/nhess-14-2749-2014.

721 Showstack, R. (2011), Threat of severe space weather to the US electrical grid explored at
722 conference, *EOS Trans.AGU*, *92*, 374-375.

723 Siscoe, G., N. U. Crooker, and C. R. Clauer (2006), Dst of the Carrington storm of 1859,
724 *Advances in Space Research*, *38*(2), 173-179, doi:https://doi.org/10.1016/j.asr.2005.02.102.

725 Smith, P. M. (1990), Effects of geomagnetic disturbances on the national grid system,
726 paper presented at 25th Universities Power Engineering Conference, Robert Gordon's
727 Institute of Technology, Robert Gordon's Institute of Technology, Aberdeen.

728 Stewart, B. (1861), On the great magnetic disturbance which extended from August 28 to
729 September 7, 1859, as recorded by photography at the Kew Observatory, *Phil.Trans.R.Soc.*,
730 *151*, 423-430, doi:10.1098/rstl.1861.0023.

731 Thomson, A. W. P., E. B. Dawson, and S. J. Reay (2011), Quantifying extreme behavior
732 in geomagnetic activity, *Space Weather-the International Journal of Research and*
733 *Applications*, *9*, 12, doi:10.1029/2011sw000696.

734 Thomson, A. W. P., A. J. McKay, E. Clarke, and S. J. Reay (2005), Surface electric fields
735 and geomagnetically induced currents in the Scottish Power grid during the 30 October 2003
736 geomagnetic storm, *Space Weather*, *3*, S11002-doi:11010.11029/12005SW000156.

737 Tol, R. S. J. (2007), The value of lost load*Rep.*, The Economic and Social Research
738 Institute (ESRI), Dublin.

739 Torta, J. M., L. Serrano, J. R. Regue, A. M. Sanchez, and E. Roldan (2012),
740 Geomagnetically induced currents in a power grid of northeastern Spain, *Space Weather-the*
741 *International Journal of Research and Applications*, *10*, 11, doi:10.1029/2012sw000793.

742 Trivedi, N. B., et al. (2007), Geomagnetically induced currents in an electric power
743 transmission system at low latitudes in Brazil: A case study, *Space Weather-the International*
744 *Journal of Research and Applications*, *5*(4), doi:10.1029/2006sw000282.

745 US - Canada Power System Outage Task Force (2006), Final report on the implementation
746 of the task force recommendations*Rep.*, Natural Resources Canada and US Department of
747 Energy.

748 Viljanen, A. (2011), European Project to Improve Models of Geomagnetically Induced
749 Currents, *Space Weather*, *9*(7), doi:doi:10.1029/2011SW000680.

Viljanen, A., A. Pulkkinen, R. Pirjola, K. Pajunpaa, P. Posio, and A. Koistinen (2006), Recordings of geomagnetically induced currents and a nowcasting service of the Finnish natural gas pipeline system, *Space Weather-the International Journal of Research and Applications*, *4*(10), doi:10.1029/2006sw000234.

Villiers, J. S., M. Kosch, Y. Yamazaki, and S. Lotz (2017), Influences of various magnetospheric and ionospheric current systems on geomagnetically induced currents around the world, *Space Weather*, *15*(2), 403-417, doi:doi:10.1002/2016SW001566.

Wang, K.-R., L. I. U. Lian-guang, and L. I. Yan (2015), Preliminary Analysis on the Interplanetary Cause of Geomagnetically Induced Current and Its Effect on Power Systems, *Chinese Astronomy and Astrophysics*, *39*(1), 78-88, doi:http://dx.doi.org/10.1016/j.chinastron.2015.01.003.

Watari, S. (2015), Estimation of geomagnetically induced currents based on the measurement data of a transformer in a Japanese power network and geoelectric field observations, *Earth Planets and Space*, *67*, 12, doi:10.1186/s40623-015-0253-8.

Wik, M., R. Pirjola, H. Lundstedt, A. Viljanen, P. Wintoft, and A. Pulkkinen (2009), Space weather events in July 1982 and October 2003 and the effects of geomagnetically induced currents on Swedish technical systems, *Annales Geophysicae*, *27*(4), 1775-1787.

769

Region	Country	Possible Rationale for assessment	Possible Grid resilience assessment
Australasia	Australia (main grid)	Applies to tree structure in main grid in east and south of Australia, particularly parts in Victoria, South Australia and Tasmania which are assessed to have significant vulnerabilities. Neglect separate grids and local generation in Western Australia and Northern Territory.	Low
	New Zealand	Good engagement from system operator, e.g. as in measures taken during the Halloween 2003 storm and following space weather damage to a transformer in 2001	High
North America	Canada (Quebec)	Highly engaged system operator	High
	US	Highly fragmented grid operation	Low
Asia	China	Extensive modern grid with many very high voltage lines. Large GICs reported in some regions, even on southern coast. Scientific publications indicate very high interest in research/power engineering community.	Low (at the moment)
	India	Highly stressed system. Conventional geomagnetic storm effects may be rare at low latitude of India, but these effects would have major impact on those rare occasions. Sudden impulse effects due to arrival of a large fast CME would affect India if that arrival was near local noon in India.	Low
	Japan	Historically thought to be at low risk of GIC due to low geomagnetic latitude. But was formally recognised as significant risk in 2015 and subject of ongoing studies.	Low (at the moment)
	Russia	Much of the grid has a tree-like structure, and some parts are at relatively high latitudes	Low
Scandinavia	Finland	High awareness in national community; also choice of transformer designs has greatly reduced risks	High
	Norway	Extensive local power generation from hydro	High
	Sweden	High awareness in national community	High
Western Europe[a]	France	The mesh structure of the French grid is a significant technical advantage, but perceived poor engagement of operators remains concerning.	Low
	Belgium	Significant dependence on France	Low
	Germany	Good mesh structure should give high resilience, but significant dependence on France, especially when renewable power is low (nighttime and lack of wind)	Low
	Netherlands	Interconnected with Germany	Low
	Denmark	Strongly interconnected with Germany	Low
	Italy	Significant dependence on France	Low
	Switzerland	Substantial resources (nuclear, hydro), some dependence on France	High
	UK (GB)	Good mesh structure in grid; high engagement from system operator and government	High
	Ireland (ROI/NI)	Growing engagement from system operator and governments	High
Africa	South Africa	Highly stressed system; extensive tree structure in grid	Low

770 Table 1 A preliminary possible assessment of power grid resilience to space weather by
771 region.

772 [a]Note that there is significant evidence that grid problems can trigger cascade failures across
773 mainland of western Europe.

774

	NO FORECAST	
	Grid resilience	
Sub-storm strength	Low	High
Very intense	Widespread power outage (50%) recovered in 72 hours; some areas (5%) without power for 6 weeks; system capacity reduced by 20% recovered in two years	Limited power outage (20%) recovered in 48 hours; some areas (5%) without power for 2 weeks; system capacity reduced by 8% recovered in 5 months
Intense	Limited power outage (10%) recovered in 72 hours; some areas (1%) without power for 4 weeks; system capacity reduced by 4% recovered in 5 months	Limited power outage (4%) recovered in 48 hours; some areas (≤1%) without power for ≤ 2 weeks
High	Limited power outage (2%) recovered in 48 hours	None
Moderate	None	None

	CURRENT FORECAST	
	Grid resilience	
Sub-storm strength	Low	High
Very intense	Widespread power outage (50%) recovered in 24 hours; some areas (5%) without power for 2 weeks; system capacity reduced by 20% recovered in two years	Limited power outage (10%) recovered in 24 hours; some areas (1%) without power for 2 weeks; system capacity reduced by 4% recovered in 5 months
Intense	Limited power outage (10%) recovered in 24 hours; some areas (1%) without power for 2 weeks; system capacity reduced by 4% recovered in 5 months	Limited power outage (2%) recovered in 24 hours
High	Limited power outage (2%) recovered in 24 hours	None
Moderate	None	None

	IMPROVED FORECAST	
	Grid resilience	
Sub-storm strength	Low	High
Very intense	Widespread power outage (20%) recovered in 24 hours; some areas (5%) without power for 2 weeks; system capacity reduced by 10% recovered in two years	Limited power outage (10%) recovered in 12 hours; some areas (1%) without power for 2 weeks; system capacity reduced by 2% recovered in 5 months
Intense	Limited power outage (4%) recovered in 24 hours; some areas (1%) without power for 2 weeks; system capacity reduced by 2% recovered in 5 months	Limited power outage (1%) recovered in 12 hours
High	None	None
Moderate	None	None

775 Table 2 Impact table based on severity of substorm and grid resilience, as well as level of

776 forecast.

Total costs (EUR m)	Immediate Recovery	No Recovery	Linear Recovery
No Forecast	M€ 12.8	M€ 668	M€ 334
Current Forecast	M€ 12.8	M€ 334	M€ 170
Improved Forecast	M€ 0.00	M€ 0.00	M€ 0.00

777

778 Table 3 Economic costs (median estimates) of space weather (in millions of Euro as of
779 August 27, 2016) for only the European substorm (#21) in the 1-in-10 year scenario under
780 different forecast and recovery assumptions.

781 Note: As described in the text, 'Immediate Recovery' assumes that the disruption, if present,
782 lasts for the duration of the substorm. 'No Recovery' assumes that there is full disruption
783 until the end of the recovery period (for example, 24 hours for Western Europe in the current
784 forecast conditions). 'Linear Recovery' assumes that the impact reduces linearly over the
785 disruption duration; mathematically this is half of the 'No Recovery' impact.

786

	No Forecast			Current Forecast			Improved Forecast		
	Immediate Recovery	Recovery After X Hours	Linear Recovery	Immediate Recovery	Recovery After X Hours	Linear Recovery	Immediate Recovery	Recovery After X Hours	Linear Recovery
Agriculture, forestry and fishing	0.18	13.11	6.55	0.18	6.55	3.41	0.00	0.00	0.00
Mining and quarrying/ electricity, gas, steam and air conditioning supply/ water supply/ sewerage/ waste management and remediation activities	0.54	7.13	3.56	0.54	3.56	1.78	0.00	0.00	0.00
Manufacturing	7.16	296.83	148.42	7.16	148.42	74.63	0.00	0.00	0.00
Construction	0.10	15.13	7.56	0.10	7.56	3.99	0.00	0.00	0.00
Wholesale and retail trade/ repair of motor vehicles and motorcycles/ transporting and storage, accommodation and food service activities	0.63	44.29	22.14	0.63	22.14	10.39	0.00	0.00	0.00
Information and communication	0.36	14.35	7.17	0.36	7.17	3.59	0.00	0.00	0.00
Financial and insurance activities	0.12	17.97	8.99	0.12	8.99	4.61	0.00	0.00	0.00
Real estate activities/ professional, scientific and technical activities/ administrative and support service activities	0.60	93.48	46.74	0.60	46.74	25.15	0.00	0.00	0.00
Public administration and defense/ compulsory social security/ education/human health and social work activities/ arts, entertainment and recreation/ other services activities	1.16	84.21	42.11	1.16	42.11	22.25	0.00	0.00	0.00
Households	1.94	81.26	40.63	1.94	40.63	20.31	0.00	0.00	0.00

Table 4 Economic costs (million EUR) to different sectors resulting from the substorm described in Table 6.

Note: Each column sums to the relevant entry in Table 6.

Total costs (EUR Bn)	Immediate Recovery	No Recovery	Linear Recovery
No Forecast	Bn € 0.18 – 0.25	Bn € 359.26 – 506.00	Bn € 89.81 – 126.50
Current Forecast	Bn € 0.18 – 0.25	Bn € 89.81 – 126.50	Bn € 22.46 – 31.64
Improved Forecast	Bn € 0.00 – 0.00	Bn € 0.00 – 0.00	Bn € 0.00 – 00

792

793 Table 5 Range estimates of total international spillovers across all sectors (in billion Euros as
794 of August 27, 2016) for a European substorm of high strength under different forecast and
795 recovery assumptions.

796

Total costs (EUR m)	Immediate Recovery	No Recovery	Linear Recovery
No Forecast	M€ 1,570	M€ 55,500	M€ 27,900
Current Forecast	M€ 1,510	M€ 18,300	M€ 9,340
Improved Forecast	M€ 635	M€ 7,340	M€ 3,700

797

798 Table 6 Economic costs (median estimates) of space weather (in million Euros as of August
799 27, 2016) for the two European substorms characterising the 1-in-30 year scenario under
800 different forecast and recovery assumptions, in a similar format to Table 5.

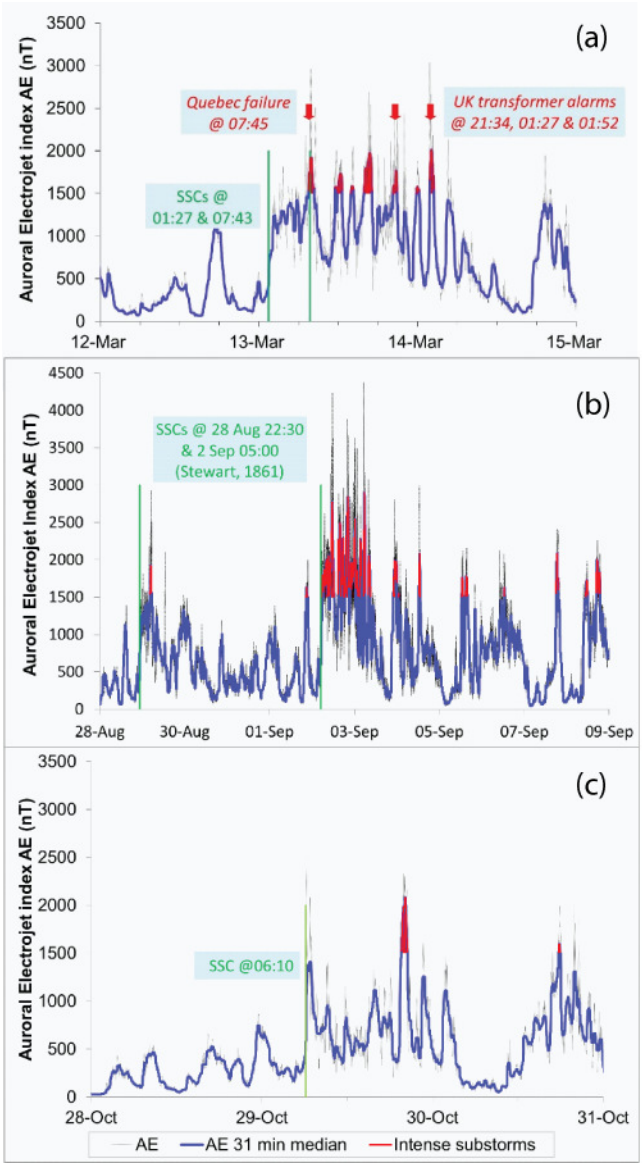
801

	No Forecast			Current Forecast			Improved Forecast		
	Immediate Recovery	Recovery After X Hours	Linear Recovery	Immediate Recovery	Recovery After X Hours	Linear Recovery	Immediate Recovery	Recovery After X Hours	Linear Recovery
Agriculture, forestry and fishing	37.00	1,796.12	909.82	36.26	596.50	310.37	14.86	237.83	122.60
Mining and quarrying/ electricity, gas, steam and air conditioning supply/ water supply/ sewerage/ waste	25.12	578.74	289.37	23.61	189.17	94.59	10.32	76.52	38.26
Manufacturing	666.52	20,929.86	10,492.63	646.03	6,918.31	3,487.32	269.67	2,772.53	1,385.73
Construction	18.29	1,429.33	726.37	17.36	469.40	247.17	7.46	189.38	95.05
Wholesale and retail trade/ repair of motor vehicles and motorcycles/ transporting and storage,	103.69	3,863.88	1,892.99	99.56	1,273.92	596.21	42.11	509.44	235.83
Information and communication	59.66	1,385.77	692.89	56.78	455.70	227.85	24.29	182.84	91.42
Financial and insurance activities	24.09	2,081.08	1,046.04	22.82	682.67	345.43	9.84	273.07	132.78
Real estate activities/ professional, scientific and technical activities/ administrative and support service	82.47	7,540.26	3,864.70	79.97	2,494.47	1,339.90	33.32	994.66	523.50
Public administration and defense/ compulsory social security/ education/human health and social work	157.75	7,689.28	3,914.81	151.02	2,532.33	1,339.94	64.15	1,019.41	525.33
activities/ arts, entertainment and recreation/ other Households	392.83	8,213.50	4,106.75	378.88	2,710.54	1,355.27	159.28	1,087.32	546.84

Table 7 Breakdown of the results of Table 8 by sectoral groups (million EUR).

Total costs (EUR Bn)	Immediate Recovery	No Recovery	Linear Recovery
No Forecast	Bn € 481 – 677	Bn € 23,483 – 33,074	Bn € 5,871 – 8,269
Current Forecast	Bn € 51 – 71	Bn € 13,551 – 19,086	Bn € 787 – 1,108
Improved Forecast	Bn € 46 – 65	Bn € 690 – 971	Bn € 193 –272

Table 8 Economic costs (median estimates) of space weather (in billion Euros as of August 27, 2016) for European substorms #28 and #41 under different forecast and recovery assumptions. This represents all losses including those arising globally as a consequence of the international spillover.



811

812 Figure 1 (a) Time series of the AE index during the 1989 storms (grey), with a 31 minute
813 running median trace overlaid (blue). Intervals of intense substorms (AE > 1500 nT) are
814 shown in blue. The times of the sudden storm commencement is shown as well as historical
815 impacts. (b) Proposed time series for a Carrington-like 1-in-100 year event, derived from the
816 1989 observations. (c) Proposed AE time series for a 1-in-10 year event corresponding to the
817 AE index for the October 2003 storm, adjusted as described in the text.

818

819 

820 Figure 2 (a) Impact footprint of substorm 21 in the 1-in-10 year scenario (b) Impact footprint
821 of substorm 28 in the 1-in-30 year scenario (c) Impact footprint of substorm 41 in the 1-in-30
822 year scenario. Figures prepared using www.blackout-simulator.com.